



ARTICLE

Cannabidiol potentiates hyperpolarization-activated cyclic nucleotide-gated (HCN4) channels

 Dana A. Page¹  and Peter C. Ruben¹ 

Cannabidiol (CBD), the main non-psychotropic phytocannabinoid produced by the *Cannabis sativa* plant, blocks a variety of cardiac ion channels. We aimed to identify whether CBD regulated the cardiac pacemaker channel or the hyperpolarization-activated cyclic nucleotide-gated channel (HCN4). HCN4 channels are important for the generation of the action potential in the sinoatrial node of the heart and increased heart rate in response to β -adrenergic stimulation. HCN4 channels were expressed in HEK 293T cells, and the effect of CBD application was examined using a whole-cell patch clamp. We found that CBD depolarized the $V_{1/2}$ of activation in holo-HCN4 channels, with an EC_{50} of 1.6 μ M, without changing the current density. CBD also sped activation kinetics by approximately threefold. CBD potentiation of HCN4 channels occurred via binding to the closed state of the channel. We found that CBD's mechanism of action was distinct from cAMP, as CBD also potentiated apo-HCN4 channels. The addition of an exogenous PIP_2 analog did not alter the ability of CBD to potentiate HCN4 channels, suggesting that CBD also acts using a unique mechanism from the known HCN4 potentiator PIP_2 . Lastly, to gain insight into CBD's mechanism of action, computational modeling and targeted mutagenesis were used to predict that CBD binds to a lipid-binding pocket at the C-terminus of the voltage sensor. CBD represents the first FDA-approved drug to potentiate HCN4 channels, and our findings suggest a novel starting point for drug development targeting HCN4 channels.

Introduction

Cannabidiol (CBD) is the main non-psychotropic cannabinoid produced by the *Cannabis sativa* plant (Lerner, 1963). CBD has many purported effects including being antiarrhythmic, anti-inflammatory, and anticonvulsant (Hill et al., 2012; Walsh et al., 2010). As such, CBD has generated a large amount of pharmacological interest and is approved by the US Food and Drug Administration for the treatment of patients with Dravet and Lennox-Gastaut syndromes (Devinsky et al., 2017, 2018; Scheffer et al., 2021). At micromolar concentrations, CBD inhibits a variety of cardiac ion channels, including $Na_v1.5$ channels (Ghovanloo et al., 2018, 2021; Fouda et al., 2020, 2022; Fouda and Ruben, 2021; Sait et al., 2020), L-type calcium channels (Ali et al., 2015), and hERG channels (Orvos et al., 2020). The resultant changes in action potential durations have been observed in various cardiomyocyte systems (Ali et al., 2015; Orvos et al., 2020; Le Marois et al., 2020; Topal et al., 2021).

Hyperpolarization-activated cyclic-nucleotide gated-channels (HCN) are important to heartbeat initiation and the diastolic depolarization phase of the action potential in the sinoatrial node of the heart (Baruscotti et al., 2011; Wahl-Schott and Biel, 2009; Stieber et al., 2003; Fenske et al., 2020; Moosmang et al., 2001).

The primary cardiac isoform of HCN channels is known as HCN4 (Brioschi et al., 2009; Herrmann et al., 2011). HCN4 channels are tetramers. Each monomer contains six transmembrane helices (S1–S6), where S1–S4 make up a distinct voltage-sensing domain (VSD), and S5–S6 of each monomer combine to form the pore domain (Lee and MacKinnon, 2017, 2019; Saponaro et al., 2021). Additionally, HCN4 channels have two cytoplasmic domains, the C-terminal cyclic-nucleotide binding domain (CNBD) (Zagotta et al., 2003) and the N-terminal HCN domain (Lee and MacKinnon, 2017; Porro et al., 2019). These domains contribute to the potentiation of HCN4 channels by cAMP (Wainger et al., 2001; Zagotta et al., 2003; Xu et al., 2010; Akimoto et al., 2014; Porro et al., 2019; Page et al., 2020), increasing heart rate (HR) in response to the β -adrenergic response (Brown et al., 1979; DiFrancesco and Tortora, 1991; Ono et al., 1993; Schweizer et al., 2010).

CBD has been anecdotally reported to alter HR and, in other cases, have no effect on HR. In an effort to determine the molecular basis for the potential effects of CBD on HR, we measured the biophysical properties of HCN4, a voltage-gated ion channel known to play a major role in regulating HR, in the presence of CBD. We used HEK 293T cells as a heterologous expression

¹Department of Biomedical Physiology and Kinesiology, Simon Fraser University, Burnaby, Canada.

Correspondence to Peter C. Ruben: pruben@sfu.ca.

© 2024 Page and Ruben. This article is distributed under the terms of an Attribution–Noncommercial–Share Alike–No Mirror Sites license for the first six months after the publication date (see <http://www.rupress.org/terms/>). After six months it is available under a Creative Commons License (Attribution–Noncommercial–Share Alike 4.0 International license, as described at <https://creativecommons.org/licenses/by-nc-sa/4.0/>).

system for HCN4 channels to test the effects of CBD application. First, we examined increasing micromolar concentrations of CBD on holo-HCN4 channels. Next, we examined whether the effect of CBD is competitive or additive with known HCN potentiators cAMP and PI(4,5)P₂. Lastly, we used computational docking to predict potential binding sites of CBD on an HCN4 structure and targeted mutagenesis to validate these predictions. We propose that CBD potentiates HCN4 channels via novel biophysical mechanisms accomplished by binding to the C-terminal region of the VSD.

Materials and methods

Cell culture

HEK 293T cells were grown at pH 7.4 in sterile-filtered DMEM + Glutamax-I (Gibco) supplemented with 10% FBS at 37°C (5% CO₂). Cells were cotransfected with mouse HCN4 (mHCN4) and eGFP using DNAfectin 2100 (ABM). Cells were plated on sterile glass coverslips 24–48 h after transfection, and experiments were conducted at least 3 h later.

Solutions and recordings

Whole-cell patch clamp experiments were performed in extracellular solution containing (in mM) 110 NaCl, 30 KCl, 0.5 MgCl₂, 1.8 CaCl₂, and 5 HEPES titrated to pH 7.4 with NaOH. Pipettes were fabricated with a P-1000 puller (Sutter) using borosilicate glass (1.5 mm O.D.) thermally polished to a resistance of 1.5–2.5 MΩ. Pipettes were filled with intracellular solution containing (in mM) 10 NaCl, 130 KCl, 0.5 MgCl₂, 1 EGTA, and 5 HEPES, titrated to pH 7.4 with KOH. CBD was dissolved in 100% DMSO to create stock solutions of 25 mM. Cyclic AMP (cAMP) (Cayman Chemical) was dissolved in PBS (pH 7.2) to create stock solutions of 10 mM. cAMP stock solution was added to the internal solution to a final concentration of 30 μM for all holo experiments. 08:0 PI(4,5)P₂, also known as diC8 PI(4,5)P₂, was dissolved in double-distilled H₂O to create stock solutions of 0.5 mM.

Recordings were conducted at 22°C with an EPC9 amplifier using Patchmaster software (HEKA Electronic). Data were lowpass filtered at 1 kHz and digitized at 20 kHz. Leak subtraction was performed online using a P/2 procedure. Gigaohm seals were allowed to stabilize in the on-cell configuration for 1 min prior to entering the whole-cell configuration. Series resistance was <5 MΩ for all recordings. All data were acquired 5 min after entering the whole-cell configuration to allow for completion of run-down and cells were allowed to incubate for at least 5 min after drug or vehicle treatment before data collection. Data were collected as matched pairs, with control or “pre-condition” data collection first, followed by perfusion and data collection for a single CBD concentration or vehicle. Due to a small volume of diC8 PI(4,5)P₂ stock solution, pre-conditions and perfusion were not performed, opting instead for a standard bath solution of extracellular solution as described above with both 10 μM diC8 PI(4,5)P₂ and 5 μM CBD.

Analysis and statistics

To determine the voltage dependence of activation, we measured tail-current amplitude at –100 mV after stepping from –40 mV to test pulse voltages ranging from either –40 to

–140 mV (holo-HCN4 channels) or –50 to –150 mV (apo-HCN4 channels) in increments of 20 mV for 2 s. Membrane potential was stepped to 0 mV after tail-current measurement for 0.5 s to allow for channel deactivation. Leak-subtracted and normalized tail-current amplitudes (*I*) were plotted versus activation voltage (*V*) and were fit with the Boltzmann function:

$$I = y_0 + a / (1 + e^{-(V-V_{1/2})/k_B T}).$$

Change in *V*_{1/2} ($\Delta V_{1/2}$) was calculated by comparing *V*_{1/2} after treatment to *V*_{1/2} before treatment. Average $\Delta V_{1/2}$ was fit to the Hill equation:

$$\Delta V_{1/2} = \text{base} + (\text{max} - \text{base}) / [1 + (X_{1/2}/X)^h].$$

Activation time constants (τ) were calculated using an iterative fit procedure with a single exponential fit equation:

$$I = Ae^{-t/\tau} + C.$$

Use dependence was determined using a 1/3 Hz protocol (20 sweeps) that stepped from the holding potential of –40 mV to –120 mV for 2 s, followed by tail-current at –100 mV. Membrane potential was stepped to 0 mV after tail current for 0.5 s. To examine the activation of mHCN4 Q401R, we stepped from the holding potential of –40 mV to –120 mV for 4 and 8 s followed by a step to 0 mV to close the channel for 0.5 s.

All statistical analyses were computed using Igor Pro software (WaveMetrics). Statistical analysis of matched pair conditions was done with a paired Student's *t* test. Statistical analysis across different conditions consisted of either one-way ANOVA followed by post-hoc Tukey's test or unpaired Student's *t* tests. For all analyses, *P* < 0.05 was considered statistically significant. Values are written as mean ± SEM, where *n* ≥ 4.

Computational docking

Computational docking was performed using AutoDock Vina (Trott and Olson, 2010; Eberhardt et al., 2021) with the published cryoEM structure of rabbit HCN4 (PDB ID 7NP4) and CBD (Drug-Bank access DB09061). Two different search space volumes were used, both >27,000 Å³, large enough to include the entirety of the transmembrane region of either a single monomer or the entire tetramer. The entire tetramer was used to examine potential binding sites at interfaces between the monomers. To account for the large search space volume, the exhaustiveness parameter was increased from the default of 8 to 100 for the monomer and 1,000 for the tetramer. The output was the nine highest affinity binding sites calculated, with multiple general locations having multiple predicted binding conformations. In the tetramer, sites were also repeated across the different monomers of the channel (Fig. S3).

Molecular biology

The Q401R mutation was introduced into the pCDNA3.1 mHCN4 plasmid (provided by the laboratory of Dr. C. Proenza, University of Colorado School of Medicine, Aurora, CO, USA) using the QuikChange Lightning Mutagenesis Kit (Agilent). The presence of the mutation was verified with Sanger sequencing (Genewiz), and successfully mutated plasmids were purified using CompactPrep Midi Prep Kit (Qiagen).

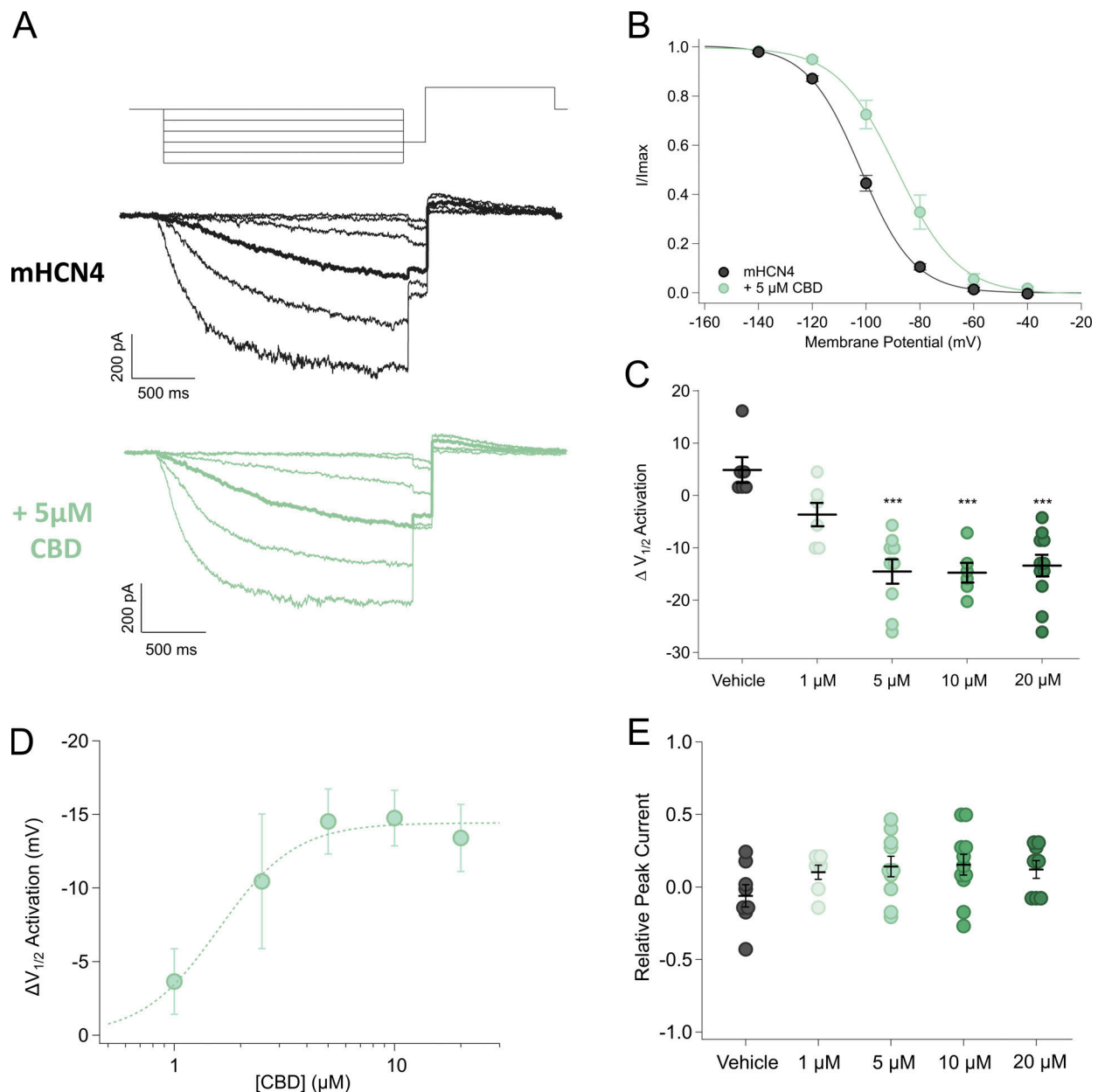


Figure 1. Effect of CBD on activation of holo-HCN4 channels. (A) Representative voltage protocol and activation current traces for mHCN4 construct before (black) and after (green) treatment with 5 μ M CBD. The -100 mV trace is highlighted. (B) Average tail current values for treatment for mHCN4 before (black) and after application of 5 μ M CBD (green). Values fit to a Boltzmann curve. Average $V_{1/2}$ for mHCN4 was -102.1 ± 1.1 ($n = 9$); average $V_{1/2}$ for 5 μ M CBD was -87.5 ± 3.0 mV ($n = 9$). (C) Scatterplot of a shift in average $\Delta V_{1/2} \pm$ SEM for the vehicle (black) and increasing concentrations of CBD (green). One-way ANOVA and post-hoc Tukey's test found a significant shift for 5, 10, and 20 μ M CBD (***) versus the vehicle ($P < 0.0001$) and 1 μ M CBD ($P < 0.03$). (D) $\Delta V_{1/2}$ of activation after treatment with various concentrations of CBD. Data were fit with the Hill equation. EC_{50} was 1.59 ± 0.21 μ M with a slope of 2.50 ± 0.63 . (E) Relative peak current from the end of activation epoch ($I_{post-treatment}/I_{pre-treatment}$) for the vehicle (black) and increasing concentrations of CBD (green). One-way ANOVA and post-hoc Tukey's test found no significant differences in relative current levels after treatments ($P > 0.2$).

Online supplemental material

Fig. S1 shows verification of the effect of cAMP on mHCN4 channels. Fig. S2 details a comparison of fitting single versus double exponential equations to holo-HCN4 channels. Fig. S3 shows alternative outputs from AutoDock Vina computation docking experiments. Fig. S4 shows additional examples of the HCN4 Q401R mutant activation with before and after CBD application superimposed. Fig.

S5 shows computational docking results between HCN4 and cholesterol.

Results

CBD shifts voltage dependence of mHCN4 channels

We measured the activation voltage dependence of holo mHCN4 channels (i.e., in the presence of 30 μ M cAMP) (Fig. 1 A) before

Table 1. Voltage-dependent activation parameters

	Pre-treatment				Post-treatment				P value ($V_{1/2}$)
	$V_{1/2}$ (mV)	n	s	n	$V_{1/2}$ (mV)	n	s	n	
Holo HCN4									
+ Vehicle	-102.3 ± 2.0	7	8.9 ± 1.7	7	-104.1 ± 2.9	7	9.0 ± 0.69	7	0.64
+1 μM CBD	-102.5 ± 1.4	6	9.6 ± 0.64	6	-98.8 ± 1.8	6	10.3 ± 0.77	6	0.17
+2.5 μM CBD	-105.4 ± 2.5	5	9.8 ± 1.1	5	-95.0 ± 2.7	5	10.2 ± 0.72	5	0.022
+5 μM CBD	-102.1 ± 1.1	9	9.8 ± 0.55	9	-87.5 ± 3.0	9	9.8 ± 0.99	9	0.0002
+10 μM CBD	-98.2 ± 2.2	6	9.4 ± 1.3	6	-83.4 ± 1.5	6	11.3 ± 1.9	6	0.0005
+20 μM CBD	-102.7 ± 1.6	11	9.5 ± 0.8	11	-89.3 ± 2.1	11	10.2 ± 0.69	11	<0.0001
+10 μM diC8-PIP ₂ ; +5 μM CBD					-76.5 ± 3.4	5	7.9 ± 0.75	5	n/a
Apo HCN4									
+5 μM CBD	-113.2 ± 2.2	7	13.5 ± 1.5	7	-97.6 ± 2.5	7	8.7 ± 0.79	7	0.0005

Average ± S.E.M. for $V_{1/2}$ and slope values calculated from the Boltzmann function. P value given from paired t test performed for each paired condition (i.e., CBD concentration or vehicle).

(black) and after perfusion with 5 μM CBD (green). The activation voltage dependence was calculated using the Boltzmann function as described in the Materials and methods section. The average $V_{1/2}$ for mHCN4 was -102.1 ± 1.1 mV ($n = 9$) and was shifted in the depolarized direction after perfusion with 5 μM CBD to -87.5 ± 3.0 mV ($n = 9$) (Fig. 1 B). CBD did not change the slope of the activation curve (Table 1). In other words, CBD potentiated mHCN4 channels, with channels activating at weaker driving forces.

The $\Delta V_{1/2}$ was calculated with different concentrations of CBD (1–20 μM) or a vehicle (Fig. 1 C and Table 1). The $\Delta V_{1/2}$ for 1 μM CBD treatment (-3.65 ± 2.22 mV, $n = 6$) was not significantly different from that of the vehicle (1.80 ± 3.71 mV, $n = 7$). However, the $\Delta V_{1/2}$ after perfusion with 5 μM (-14.5 ± 2.2 mV, $n = 9$) was significantly different than the vehicle ($P < 0.0001$) and 1 μM CBD ($P < 0.03$). Treatment with 5 μM CBD was sufficient to exert maximal shift in $\Delta V_{1/2}$; we observed no significant increase in $\Delta V_{1/2}$ with larger concentrations of CBD (10 and 20 μM) (Table 1). Using the Hill equation (Fig. 1 D), the EC_{50} of CBD was calculated to be 1.59 ± 0.21 μM, suggesting this potentiation could occur at therapeutically relevant concentrations. Additionally, the Hill slope was 2.50 ± 0.63, suggesting positive binding cooperativity between multiple binding sites.

Previous studies found that CBD increased the current density of mHCN1 channels in intact *Xenopus laevis* oocytes (Mayar et al., 2022). To test if this was true in mHCN4 channels, we examined the relative peak current after perfusion of CBD. We compared peak current density at -120 mV, measured at the end of the activation epoch, before and after perfusion with CBD or vehicle (Fig. 1 E). We found no significant difference in the peak current density for all concentrations of CBD tested (1–20 μM) compared with the vehicle, so we concluded that CBD did not increase HCN4 current density.

CBD speeds activation of mHCN4 channels

We next examined how CBD affected the activation kinetics of mHCN4 channels. We fit the concave-down portions of the

activation sweeps with a single exponential equation, allowing us to calculate τ_{act} (Fig. 2 A). All concentrations of CBD tested significantly sped ($P < 0.04$) the activation of mHCN4 channels (Fig. 2, A and B) between -100 and -140 mV. For example, at -120 mV (Fig. 2 A), τ_{act} was 1,270 ± 160 ms ($n = 6$) after treatment with the vehicle, while τ_{act} was 404 ± 59 ($n = 8$) after treatment with 5 μM CBD, a threefold decrease in τ_{act} (Table 2). This speeding of activation is not fully accounted for by the shift in activation $V_{1/2}$ (~15 mV). To account for $\Delta V_{1/2}$, we compared τ_{act} at similar driving forces, i.e., -140 mV after treatment with vehicle and -120 mV after treatment with 5 μM CBD. At similar driving forces, 5 μM CBD still significantly (unpaired Student's t test $P < 0.02$) decreased τ_{act} by 1.5-fold. This suggests that CBD stabilizes the transition to the activated state in addition to its effect on voltage dependence.

CBD binds to the closed state of mHCN4 channels

We studied the state dependence of CBD's action on HCN4 channels by using a 1/3 Hz repetitive activation protocol to measure τ_{act} over time. The protocol was 20 sweeps, for a total of 60 s using -120 mV as the activation voltage. If CBD was bound to the open state, we would expect a decrease in τ_{act} over time as more CBD molecules bind to the open state. However, if CBD bound the closed state, we would expect a decrease in τ_{act} immediately. We found that in sweep 1, 5 μM CBD significantly decreased τ_{act} ($P < 0.02$): 940 ± 190 ms ($n = 7$) before treatment compared with 510 ± 51 ($n = 7$) after treatment (Fig. 2, C and D). This is consistent with our previous results of the effect of CBD on τ_{act} (Fig. 2 B and Table 2). The speeding of the activation did not significantly change with increasing activation sweeps (Fig. 2, C and D). After treatment with 5 μM CBD, τ_{act} for sweep 20 (435 ± 64 ms, $n = 6$) was not significantly different from τ_{act} on sweep 1 (510 ± 51 ms, $n = 7$). Combined these results suggest that CBD binds to the closed state of mHCN4.

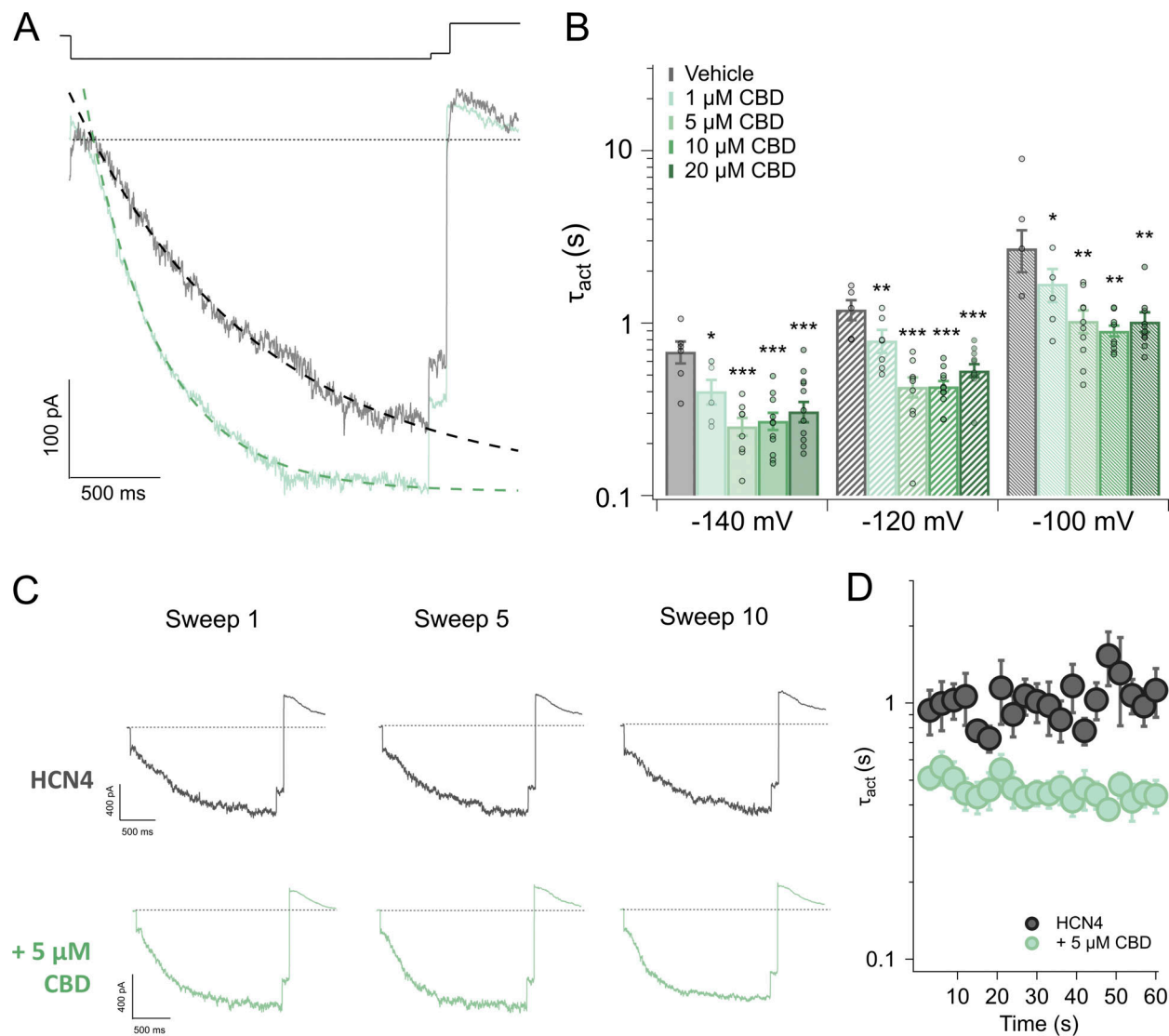


Figure 2. Effect of CBD on activation kinetics of holo-HCN4 channels. (A) Superimposition of activation epoch (–120 mV) pre- (black) and post-treatment with 5 μM CBD (green), dotted line shows 0 current. Single exponential fit of activation epochs shown in dashed lines. (B) Average activation $\tau \pm \text{SEM}$ between –140 and –100 mV. One-way ANOVA and post-hoc Tukey’s test found all concentrations of CBD significantly sped activation compared with vehicle (* $P < 0.05$; ** $P < 0.01$; *** $P < 0.001$). Additionally at –120 mV, treatment with 5–20 μM CBD significantly sped activation compared to treatment with 1 μM CBD ($P < 0.02$). (C) Use-dependence 1/3 Hz protocol at –120 mV pre (black) and posttreatment with 5 μM CBD (green), sweep 1, 5, and 10 shown. The effect of CBD does not change over time. Dotted line shows 0 current. (D) Average $\tau_{\text{act}} \pm \text{SEM}$ at –120 mV during 1/3 Hz protocol ($n = 7$), total of 20 sweeps. Unpaired Student’s t test found CBD significantly sped activation ($P < 0.03$), but that after treatment with 5 μM CBD sweep 1 τ_{act} is not significantly different than sweep 20 τ_{act} ($P > 0.2$). Thus, the effect of CBD does not change over the course of 60 s.

Mechanism for potentiation of mHCN4 channels by CBD is independent of small molecules: cAMP and PI(4,5)P₂

How does CBD potentiate HCN4 channels? We examined whether CBD was acting cooperatively with cAMP to potentiate mHCN4 channels. Similar to CBD, cAMP speeds activation and shifts the $V_{1/2}$ of mHCN4 channels by approximately +10 mV (Fig. S1). We measured $\Delta V_{1/2}$ after treatment with 5 μM CBD in apo channels (i.e., no cAMP was present in the internal solution) (Fig. 3 A). In the absence of cAMP, the $V_{1/2}$ was -113 ± 2.2 mV ($n = 7$), and after CBD treatment, $V_{1/2}$ was -97.6 ± 2.5 mV ($n = 7$), a $\Delta V_{1/2}$ of -15.5 ± 2.0 mV ($n = 7$) (Fig. 3 B). A comparison to results from Fig. 1 B show that in the presence of CBD, cAMP still shifts the $V_{1/2}$ by approximately +10 mV. Additionally,

CBD treatment still decreased τ_{act} by at least 1.5-fold at –130 and –150 mV (Table 2) in apo-HCN4 channels. Combined, this suggests that the biophysical mechanisms by which CBD and cAMP potentiate HCN4 channels are separate and independent of one another.

We next examined whether CBD was acting through a similar mechanism as the lipid PI(4,5)P₂. PI(4,5)P₂ is known to shift $V_{1/2}$ of HCN1, HCN2, and HCN4 channels by 15–20 mV (Zolles et al., 2006; Pian et al., 2006, 2007). Our previous experiments were performed after the rundown was complete, so in the absence of PI(4,5)P₂. Therefore, we examined the effect of CBD in the presence of an exogenous PI(4,5)P₂ analog diC8 PI(4,5)P₂ (Fig. 3 C). diC8 PI(4,5)P₂ is faster-acting and more

Table 2. **Activation kinetics parameters**

	$\tau_{\text{Activation}}$ (ms)					
	-140 mV	n	-120 mV	n	-100 mV	n
Holo HCN4	580 ± 42	44	1,360 ± 140	45	2,870 ± 330	30
+ Vehicle	682 ± 99	6	1,270 ± 160	5	2,550 ± 550	4
+1 μM CBD	436 ± 68	6	790 ± 100	7	1,560 ± 340	5
+5 μM CBD	256 ± 36	7	405 ± 59	8	951 ± 130	9
+10 μM CBD	271 ± 32	11	430 ± 33	11	901 ± 68	10
+20 μM CBD	357 ± 50	11	560 ± 43	11	1,020 ± 120	11
+10 μM diC8-PIP ₂ ; +5 μM CBD	319 ± 35	4	601 ± 64	5	955 ± 77	4
	-150 mV	n	-130 mV	n	-110 mV	n
Apo HCN4	430 ± 110	5	970 ± 120	7	1,471 ± 96	4
+5 μM CBD	276 ± 25	7	445 ± 37	7	1,075 ± 91	7

Average ± S.E.M. for activation τ for the three most hyperpolarized voltages measured.

soluble than PI(4,5)P₂ and shifts $V_{1/2}$ of HCN2 by 10 mV (Pian et al., 2006). The average $V_{1/2}$ after the addition of 10 μM diC8 PI(4,5)P₂ and 5 μM CBD was -76.5 ± 3.4 ($n = 5$) (Fig. 3 D), a further depolarizing shift of ~ 10 mV compared with $V_{1/2}$ after treatment with 5 μM CBD (Fig. 1 B and Table 1). This suggests that although CBD and PI(4,5)P₂ are both lipophilic small molecules, they use unique biophysical mechanisms to potentiate HCN4 channels.

CBD is predicted to interact with the VSD

To give us further insight into the mechanism CBD utilizes to potentiate HCN4, we performed computational docking of CBD with the cryoEM structure of HCN4. Using AutoDock Vina, we identified nine of the highest affinity binding sites for both a single HCN4 monomer and the full tetramer (highest affinity binding for tetramer shown in Fig. 4, A-D). Cytosolic domains were excluded due to the lipophilic nature of CBD (ClogP = 6.33 [Chemaxon]). Of particular interest was a binding pocket in the center of the VSDs (Fig. 4, A and B), where CBD binding events clustered in the experiments for the monomer and tetramer. This pocket was previously identified as a lipid-binding pocket of unknown effect (Saponaro et al., 2021). CBD binding here would position it in a prime location to modulate voltage sensor movement (Fig. 4, C and D), agreeing with our functional data. To test if CBD binds here, we introduced an arginine at the Q401 position (Fig. 4, D and E). The voltage dependence of the HCN4 Q401R mutant was drastically shifted to hyperpolarized potentials and activation was surprisingly slow, resulting in a linear curve even when activation time was increased up to 8 s (Fig. S4). As such, we were unable to measure activation $V_{1/2}$ or calculate τ_{Act} . Application of 5 μM CBD had no visual effect on

the activation of HCN4 Q401R (Fig. 4 E and Fig. S4), suggesting that the activity of CBD was disrupted. This supports the hypothesis that CBD affects HCN4 channels by binding to the binding pocket identified via computational docking.

Discussion

CBD is a highly promiscuous small molecule, interacting with a variety of transmembrane proteins and ion channels. In general, CBD blocks many of the ion channels it interacts with, including all subtypes of Na_v channels, K_v1.2, KCNQ1/KCNE1 channels, L-type calcium channels, and the HCN relative, the hERG channel (Ali et al., 2015; Ghovanloo et al., 2018; Orvos et al., 2020; Isaev et al., 2022; Topal et al., 2021). Recently, CBD has been shown to potentiate some neuronal channels: increasing the current density of HCN1 channels (Mayar et al., 2022) and activating K_v7 channels by shifting the voltage dependence at submicromolar concentrations (Zhang et al., 2022). Our results show that CBD is the first FDA-approved drug to potentiate cardiac HCN channels by modulating HCN4 voltage dependence and activation kinetics.

Functional evidence for mechanism of action

We propose that CBD binds to HCN4 channels (Fig. 5) resulting in both depolarization of the $V_{1/2}$ of activation and speeding of activation kinetics. Thus, CBD allows HCN4 channels to open at weak driving forces. We calculated the $V_{1/2}$ from a fixed activation epoch time for all voltages, which is not a true steady state. Steady-state $V_{1/2}$ values may be more depolarized than the isochronal $V_{1/2}$ values found here. However, the effect of CBD on $V_{1/2}$ is expected to be preserved at true steady state as well as its effect on activation kinetics. We found that the shift in $V_{1/2}$ after CBD application did not result in a significant increase in the current density of HCN4 channels. In contrast, Mayer et al. (2022) found that in intact oocytes, CBD increased the current density of HCN1 channels without shifting the voltage dependence of activation. This difference could be due to the use of intact oocytes versus the HEK 293T cells used in this study. Alternatively, the distinct responses to CBD could be due to isoform-specific differences in HCN1 and HCN4 channels. HCN1 and HCN4 differ in both activation kinetics, thought to be due to sequence differences in the S2 helix, as well as the response to cAMP (Moosmang et al., 2001; Chen et al., 2001; Wang et al., 2001; Lolicato et al., 2011). Combined, the result is HCN1 channels activating at more depolarized potentials than HCN4 channels. Thus, the distinct responses to CBD could be due to these inherent differences in HCN isoforms.

The EC₅₀ for $\Delta V_{1/2}$ was 1.59 μM and, although the EC₅₀ for the decrease in τ_{act} was unable to be calculated with the concentrations of CBD used, we expect it to be < 1 μM . Thus, we expect that CBD can potentiate HCN4 channels at therapeutically relevant concentrations. The calculated Hill slope for $\Delta V_{1/2}$ was > 1 , indicating multiple binding sites. Since HCN4 channels are tetramers, logic suggests that there would be up to four binding sites present in homomeric channels. Based on the Hill slope, we suggest that at least two CBD molecules bind to potentiate HCN4 channels. Future work could examine the exact number of CBD

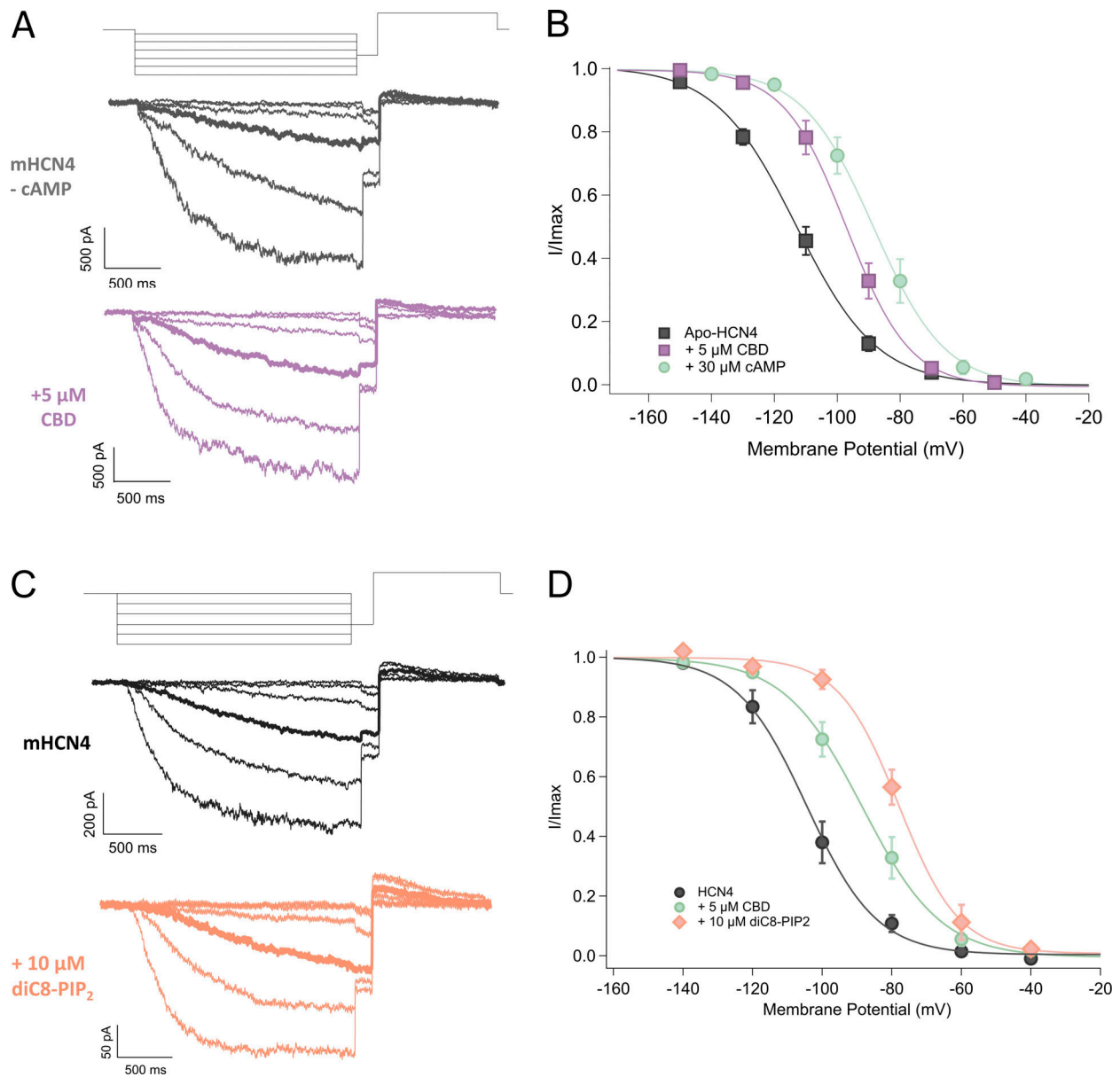


Figure 3. **CBD potentiation is distinct from cAMP and PIP₂.** (A) Representative voltage protocol and traces of mHCN4 in the absence of cAMP before (black) and after (purple) treatment with 5 μM CBD. The -100 mV trace is highlighted. (B) Average tail current values for pre- (black square) and post-treatment with 5 μM CBD (purple square) in the absence of cAMP (apo-HCN4 channels), and treatment with 5 μM CBD in the presence of cAMP (green circle). Values were fit to the Boltzmann function. Average $V_{1/2}$ for pre-treatment (black square) was -113.2 ± 2.2 mV ($n = 7$); average $V_{1/2}$ for post-treatment with 5 μM CBD (purple square) was -97.6 ± 2.5 mV ($n = 7$); average $V_{1/2}$ for post-treatment with 5 μM CBD in presence of cAMP (green circle) was -87.5 ± 3.0 mV ($n = 9$). One-way ANOVA and post-hoc Tukey's test found that the application of CBD significantly shifted $V_{1/2}$ ($P < 0.003$) by ~ 15 mV, and the presence of cAMP and CBD significantly shifted $V_{1/2}$ ($P < 0.04$) a further 10 mV. (C) Representative traces of mHCN4 (black) and mHCN4 after application of diC8-PI(4,5)P₂ (orange). The -100 mV trace is highlighted. (D) Average tail current values for treatment with vehicle (black circle), 5 μM CBD (green circle), and 5 μM CBD with 10 μM diC8-PI(4,5)P₂ (orange diamond). Values fit to the Boltzmann function.

molecules required and whether increasing numbers of CBD molecules bound increases the potentiation effect.

Activation kinetics were calculated using a single exponential fit. Residuals of single and double exponential fits were compared at the three voltages (Fig. S2); single exponentials were sufficient to accurately model the activation kinetics. It must be noted that at more depolarized potentials, the accuracy of the τ_{Act} will be decreased. As such, τ_{Act} values described in this work from -100 mV may be faster than the true speed. While our

results from the repetitive pulse protocol suggest that CBD binds to the closed state, we have not excluded the idea that CBD doesn't have state dependence, binding to closed- or open-state with no change in affinity, or that the CBD on-rate is too fast to be accurately measured by this analysis. Future work could be done to determine whether the effects of CBD are caused by binding to and destabilizing the HCN4 closed state.

CBD's potentiation was additive to the activities of both cAMP and PI(4,5)P₂, suggesting a unique biophysical mechanism from

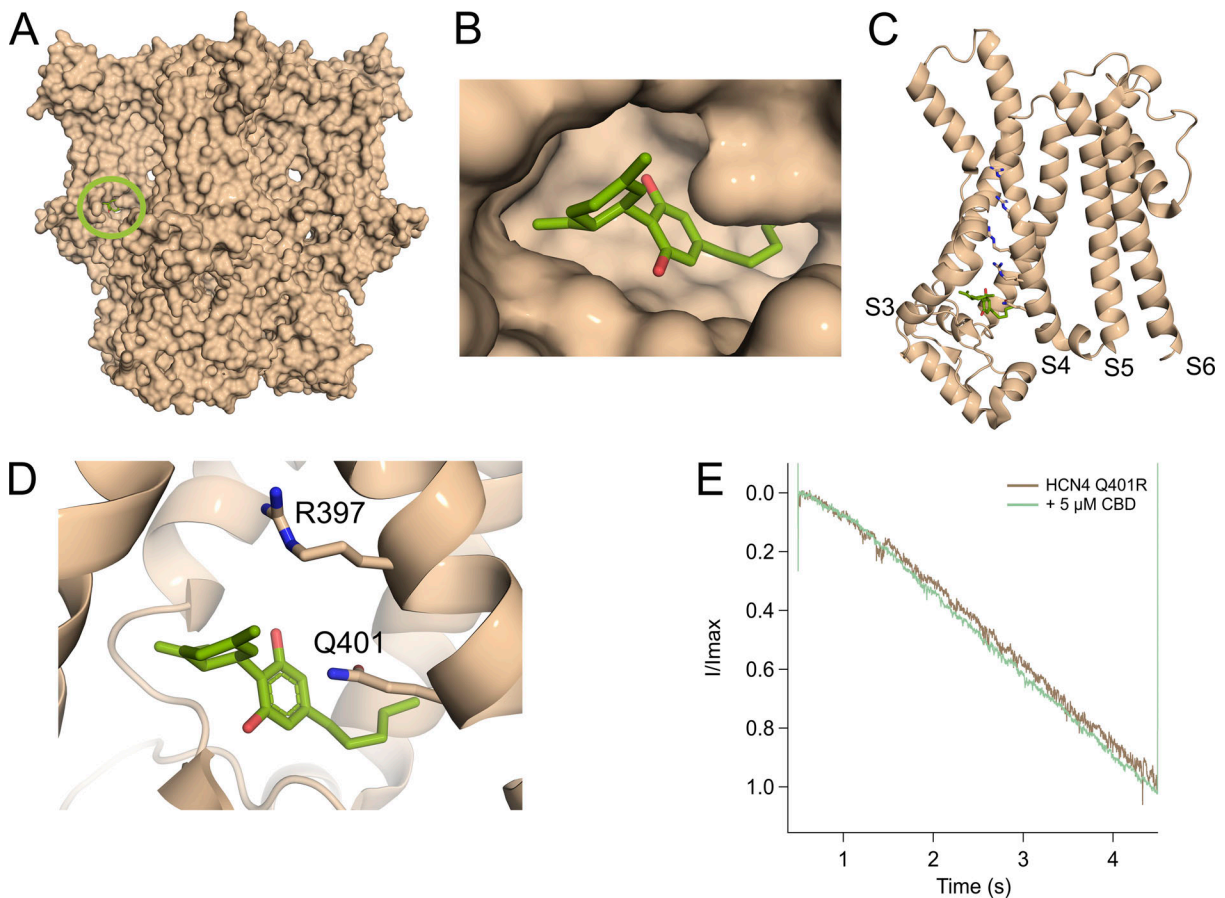


Figure 4. **Computed highest binding affinity binding site of CBD with the cAMP bound HCN4 structure.** (A) Space-fill model of HCN4, CBD (green) highlighted by green circle. (B) Zoomed in view of lipid binding pocket bound by CBD. (C) CBD binding location in the VSD of one subunit. (D) CBD is predicted to be in close proximity to polar (Q401) and charged (R397) residues of S4. (E) Normalized superimposition of HCN4 Q401R activation epoch before (brown) and after application of 5 μ M CBD (green) for representative trace.

these two small molecules. cAMP relieves the autoinhibition of HCN4 channels. We tested if CBD acts using a common mechanism as cAMP but found that CBD potentiation was distinct from cAMP. However, since CBD was not tested on a channel incapable of autoinhibition (i.e., without the CNBD), we cannot definitively conclude that CBD does not also relieve autoinhibition in a non-competitive way to cAMP. Claveras Cabezudo et al. (2022) performed computational modeling to predict that phosphoinositides bind to the surface of the HCN domain along with S2 and S3 helices. Our mutational and docking studies do not predict that CBD binds to similar locations (Fig. S3) (Claveras Cabezudo et al., 2022). Thus, our findings that CBD and PI(4,5)P₂ have unique biological functions agree with the predicted binding sites of these molecules.

Computational binding predictions for CBD

The highest affinity binding site computed for CBD is located in a lipid binding pocket at the C-terminus of the VSD. Binding here places CBD close to the charged residues of the voltage sensor (Fig. 5), a prime position from which to regulate HCN4 activation voltage dependence. This pocket was bound to a lipid in the cryoEM structure (Saponaro et al., 2021), and with

computational docking we found that cholesterol was also predicted to bind in this pocket (Fig. S5). Combined, this suggests that this pocket is a general lipid binding site, where lipids or highly lipophilic molecules like CBD bind primarily using van der Waals and hydrophobic interactions with the S2–S3 linker.

The results of the computational binding analysis also suggested alternative binding sites, some repeated in multiple monomers of the channels (Fig. S3). The most common alternative site was on the surface of the channel, against the C-terminus of the S1 helix. While the N-terminus of the HCN4 S1 helix is implicated in channel gating via interactions with the S4 helix (Ishii et al., 2007; Ramentol et al., 2020), the C-terminal S1 residues have not been implicated in gating. As such, CBD binding here is less likely to produce the observed potentiation than the proposed lipid-binding pocket (Fig. 4).

Mutagenesis to examine the binding site of CBD produced a channel, HCN4 Q401R, with drastically shifted activation voltage dependence and slowed activation kinetics. Increasing the time of the activation epoch (2 s) by two- and fourfold still resulted in a linear trace that was unable to be fit by a single exponential equation (Fig. S4). As such, we chose to qualitatively observe if CBD sped activation kinetics via superimposition of activation

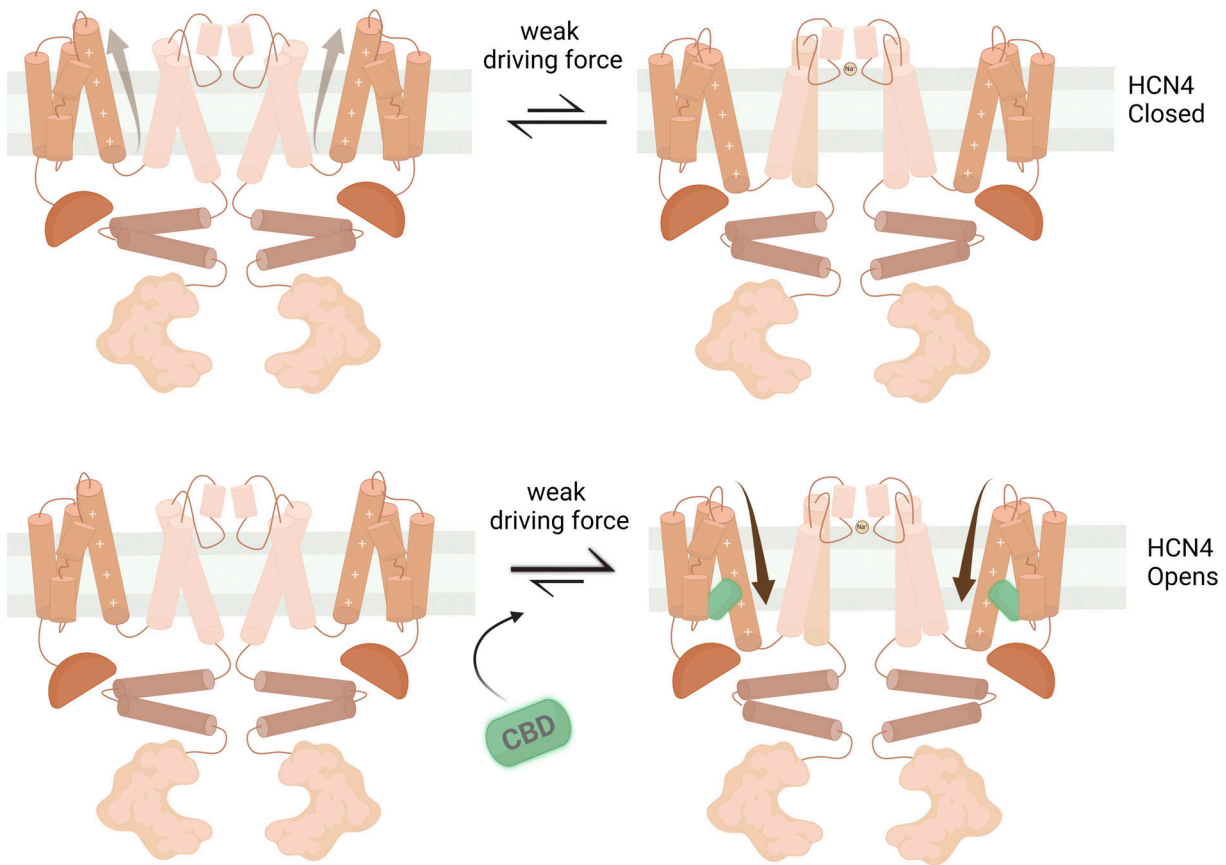


Figure 5. **Schematic for the mechanism of action of CBD (green) on HCN4 channels.** Top: Under normal physiological conditions, HCN4 channels would not open at weak driving forces (i.e., -80 mV). Bottom: When CBD is added, it stabilizes the S4 in the activated state, allowing HCN4 channels to open at weak driving forces. Figure created with <https://BioRender.com>.

traces. Application of $5 \mu\text{M}$ CBD did not have a qualitative effect on activation, with no substantial change in the linear curve being observed (Fig. 4 E and Fig. S4) across eight different cells. We concluded from this that the Q401R mutation disrupted the binding of CBD, possibly by increasing the polarity of the binding site. This result provides secondary evidence that CBD binds near Q401, in the proposed binding pocket at the C-terminus of the VSD.

The classical gating charge transfer centers were originally documented in the crystal structure of a $K_v1.2$ - $K_v2.1$ chimera and are conserved in HCN4 channels (Tao et al., 2010; Saponaro et al., 2021). Gating charge transfer centers are composed of three residues: a phenylalanine and two negatively charged residues. The phenylalanine acts in two ways: (1) to block or “cap” the gating pathway, and (2) to stabilize the gating charges via cation- π interactions. These cation- π interactions preferentially bind to lysine over arginine residues, promoting inward movement of the voltage sensor. CBD contains a benzene ring located near gating charges when bound to the proposed binding pocket. Similar to the phenylalanine of the gating charge transfer center, cation- π interactions between gating charges and CBD could promote the inward movement of the voltage sensor. Specifically, in the closed state, the glutamine at the C-terminal end of S4 is closest to CBD. We propose that the benzene ring would

preferentially bind to the arginine one helical turn away, resulting in the observed potentiation and promoting the inward motion of the S4 helix.

Comparison of CBD's action on HCN4 channels to other drugs and small molecules

HCN channels have long been targets for drug development. Ivabradine, a common treatment for chronic heart failure, is an HCN-specific channel blocker that binds to the open state of the channel (Bucchi et al., 2013; Postea and Biel, 2011). Additional blockers have also been developed, although not approved for use in patients, including other imidazolines like alinidine and zatebradine, and the piridinium derivative ZD7288 (Postea and Biel, 2011; Novella Romanelli et al., 2016). Unfortunately, none of these drugs were found to be specific to HCN channels. Unlike these drugs, CBD does not block HCN channels, and as such represents a novel starting point for future drug development.

CBD is not the first natural product that has been found to potentiate HCN channels. The flavonoid fisetin and the phytoestrogen isoflavonoid genistein, both plant metabolites, have been shown to potentiate the related HCN2 channels (Carlson et al., 2013; Rozario et al., 2009). These compounds competed with cAMP via binding to the cAMP binding pocket, while the action of CBD was unaffected by the presence or absence of cAMP. Tanshinone IIA is a lipophilic constituent of the Chinese

medicinal herb *Salvia miltiorrhiza*, also known as Danshen, that is used in traditional medicine to treat cardiovascular disease. Similar to CBD, tanshinone IIA possesses a myriad of activities, including being cardioprotective, neuroprotective, and anti-inflammatory. Tanshinone IIA has a mixed effect on HCN1 and 2, increasing channel open probability while slowing activation and deactivation (Liang et al., 2009). Since CBD potentiates HCN4 channels by shifting voltage dependence and speeding activation, it must contain novel features or functional groups compared with these three plant metabolites.

HCN channels have been found to be regulated by a variety of human-derived lipids, including phosphoinositides (Pian et al., 2006, 2007; Zolles et al., 2006; Flynn and Zagotta, 2011). While we found that CBD acts in a distinct mechanism from PI(4,5)P₂, two other acidic phospholipids present in human cells, phosphatidic acid (PA) and arachidonic acid (AA), directly modulate HCN1 and HCN2 channels (Fogle et al., 2007). PA and AA both depolarize the V_{1/2}, like CBD; however, AA also decreases the open probability of the channels, which CBD does not. Future work could be done to examine if CBD utilizes a common biophysical mechanism with PA and AA. Another lipid that regulates HCN channels is cholesterol (Fürst and D'Avanzo, 2015). Cholesterol regulates the main HCN channel isoforms (HCN1, HCN2, and HCN4) in distinct ways. With HCN4 channels, cholesterol facilitates mode-shift, a mechanism where channels display hysteresis in their voltage dependence, having a more stable open state if they have been exposed to activating voltage previously. While cholesterol may bind in a similar location as CBD (Fig. S5), clearly the structural features of these two molecules elicit very different effects on HCN4 channels.

Physiological implications

In humans, use of cannabis results in a short-term increase in heart rate by up to 50 beats per minute (Beaconsfield et al., 1972; Jones, 2002). HCN4 channels play a prominent role in the initiation of the diastolic depolarization phase of action potentials in the SA node (Brown et al., 1979; DiFrancesco and Tortora, 1991). Thus, activation of HCN4 channels by CBD would accelerate the heart rate, partially explaining this phenomenon. Previous studies on CBD effects on action potential duration (APD) have noted both shortening and lengthening of APDs depending on the organism used (Orvos et al., 2020; Le Marois et al., 2020; Isaev et al., 2022). However, no increase in QT intervals was reported in clinical trials of CBD in humans (Stanley et al., 2013; Iffland and Grotenhermen, 2017). CBD's potentiation of HCN4 channels could play a role in this as HCN isoforms including HCN4 are expressed in ventricular cardiomyocytes (Shi et al., 1999; Zhang et al., 2009). Potentiation of HCN4 would result in outward current during the plateau phase of the ventricular action potential counteracting the inhibition of other cardiac potassium channels like I_{Kr} (hERG) and I_{Ks} (Ueda et al., 2009; Orvos et al., 2020; Topal et al., 2021). Various heterozygous HCN4 channelopathies in humans have been identified with the phenotype for most patients including bradycardia (Postea and Biel, 2011). Additionally, common medications like β-blockers (atenolol), verapamil, and digitalis can induce sinus node dysfunction (Margolis et al., 1975; Strauss et al., 1976;

Breithardt et al., 1978; Manne, 2018). Our results suggest that CBD could be a novel platform for drug development to protect against bradycardia and sinus dysfunction resulting from familial mutations or drug-induced.

Data availability

The data used to generate tables and figures are openly available in the publicly accessible database: Summit Research Repository at <https://summit.sfu.ca/item/36669>.

Acknowledgments

Jeanne M. Nerbonne served as editor.

We thank Dr. C. Proenza for the generous donation of the mHCN4 construct.

This work was supported by the Natural Sciences and Engineering Research Council of Canada to P.C. Ruben (RPGIN03920) and by a MITACS Elevate grant in partnership with Akseera Pharma, Inc. to D.A. Page (IT21730).

We acknowledge that our MITACS partner is a pharmaceutical company interested in cannabis, but this fact did not affect our findings and the authors have no financial interest in the partner company. Akseera Pharma, Inc. was not involved in the study design, collection, analysis, interpretation of data, the writing of this article, or the decision to submit it for publication.

Author contributions: D.A. Page and P.C. Ruben conceptualized the experiments. D.A. Page collected, analyzed, interpreted, and visualized the data, and wrote the first draft of the manuscript. P.C. Ruben provided project administration and resources, as well as critical review and revision of the manuscript.

Disclosures: D.A. Page reported grants from Akseera Pharma Corp during the conduct of the study. P.C. Ruben reported grants from MITACS/Akseera Pharma, Inc. during the conduct of the study.

Submitted: 10 November 2023

Revised: 15 March 2024

Accepted: 9 April 2024

References

- Akimoto, M., Z. Zhang, S. Boulton, R. Selvaratnam, B. VanSchouwen, M. Gloyd, E.A. Accili, O.F. Lange, and G. Melacini. 2014. A mechanism for the auto-inhibition of hyperpolarization-activated cyclic nucleotide-gated (HCN) channel opening and its relief by cAMP. *J. Biol. Chem.* 289:22205–22220. <https://doi.org/10.1074/jbc.M114.572164>
- Ali, R.M., L.T. Al Kury, K.H.S. Yang, A. Qureshi, M. Rajesh, S. Galadari, Y.M. Shuba, F.C. Howarth, and M. Oz. 2015. Effects of cannabidiol on contractions and calcium signaling in rat ventricular myocytes. *Cell Calcium.* 57:290–299. <https://doi.org/10.1016/j.ceca.2015.02.001>
- Baruscotti, M., A. Bucchi, C. Viscomi, G. Mandelli, G. Consalez, T. Gnecci-Rusconi, N. Montano, K.R. Casali, S. Micheloni, A. Barbuti, and D. DiFrancesco. 2011. Deep bradycardia and heart block caused by inducible cardiac-specific knockout of the pacemaker channel gene *Hcn4*. *Proc. Natl. Acad. Sci. USA.* 108:1705–1710. <https://doi.org/10.1073/pnas.1010122108>
- Beaconsfield, P., J. Ginsburg, and R. Rainsbury. 1972. Marijuana smoking. Cardiovascular effects in man and possible mechanisms. *N. Engl. J. Med.* 287:209–212. <https://doi.org/10.1056/NEJM197208032870501>

- Breithardt, G., L. Seipel, E. Wiebringhaus, and F. Loogen. 1978. Effects of verapamil on sinus node function in man. *Eur. J. Cardiol.* 8:379–394. https://doi.org/10.1007/978-94-009-9715-8_11
- Brioschi, C., S. Micheloni, J.O. Tellez, G. Pisoni, R. Longhi, P. Moroni, R. Billeter, A. Barbuti, H. Dobrzynski, M.R. Boyett, et al. 2009. Distribution of the pacemaker HCN4 channel mRNA and protein in the rabbit sinoatrial node. *J. Mol. Cell. Cardiol.* 47:221–227. <https://doi.org/10.1016/j.yjmcc.2009.04.009>
- Brown, H.F., D. DiFrancesco, and S.J. Noble. 1979. How does adrenaline accelerate the heart? *Nature.* 280:235–236. <https://doi.org/10.1038/280235a0>
- Bucchi, A., M. Baruscotti, M. Nardini, A. Barbuti, S. Micheloni, M. Bolognesi, and D. DiFrancesco. 2013. Identification of the molecular site of ivabradine binding to HCN4 channels. *PLoS One.* 8:e53132. <https://doi.org/10.1371/journal.pone.0053132>
- Carlson, A.E., J.C. Rosenbaum, T.I. Brelidze, R.E. Klevit, and W.N. Zagotta. 2013. Flavonoid regulation of HCN2 channels. *J. Biol. Chem.* 288:33136–33145. <https://doi.org/10.1074/jbc.M113.501759>
- Chen, J., J.S. Mitcheson, M. Tristani-Firouzi, M. Lin, and M.C. Sanguinetti. 2001. The S4-S5 linker couples voltage sensing and activation of pacemaker channels. *Proc. Natl. Acad. Sci. USA.* 98:11277–11282. <https://doi.org/10.1073/pnas.201250598>
- Claveras Cabezedo, A., A. Feriel Khoualdi, and N. D'Avanzo. 2022. Computational prediction of phosphoinositide binding to hyperpolarization-activated cyclic-nucleotide gated channels. *Front. Physiol.* 13:859087. <https://doi.org/10.3389/fphys.2022.859087>
- Devinsky, O., J.H. Cross, L. Laux, E. Marsh, I. Miller, R. Nabbut, I.E. Scheffer, E.A. Thiele, S. Wright, and Cannabidiol in Dravet Syndrome Study Group. 2017. Trial of cannabidiol for drug-resistant seizures in the Dravet syndrome. *N. Engl. J. Med.* 376:2011–2020. <https://doi.org/10.1056/nejmoa1611618>
- Devinsky, O., A.D. Patel, J.H. Cross, V. Villanueva, E.C. Wirrell, M. Privitera, S.M. Greenwood, C. Roberts, D. Checketts, K.E. VanLandingham, et al. 2018. Effect of cannabidiol on drop seizures in the lennox-gastaut syndrome. *N. Engl. J. Med.* 378:1888–1897. <https://doi.org/10.1056/nejmoa1714631>
- DiFrancesco, D., and P. Tortora. 1991. Direct activation of cardiac pacemaker channels by intracellular cyclic AMP. *Nature.* 351:145–147. <https://doi.org/10.1038/351145a0>
- Eberhardt, J., D. Santos-Martins, A.F. Tillack, and S. Forli. 2021. AutoDock Vina 1.2.0: New docking methods, expanded force field, and python bindings. *J. Chem. Inf. Model.* 61:3891–3898. <https://doi.org/10.1021/acs.jcim.1c00203>
- Fenske, S., K. Hennis, R.D. Rötzer, V.F. Brox, E. Becirovic, A. Scharr, C. Gruner, T. Ziegler, V. Mehlfeld, J. Brennan, et al. 2020. cAMP-dependent regulation of HCN4 controls the tonic entrainment process in sinoatrial node pacemaker cells. *Nat. Commun.* 11:5555. <https://doi.org/10.1038/s41467-020-19304-9>
- Flynn, G.E., and W.N. Zagotta. 2011. Molecular mechanism underlying phosphatidylinositol 4,5-bisphosphate-induced inhibition of SpIH channels. *J. Biol. Chem.* 286:15535–15542. <https://doi.org/10.1074/jbc.M110.214650>
- Fogle, K.J., A.K. Lyashchenko, H.K. Turbendian, and G.R. Tibbs. 2007. HCN pacemaker channel activation is controlled by acidic lipids downstream of diacylglycerol kinase and phospholipase A2. *J. Neurosci.* 27:2802–2814. <https://doi.org/10.1523/JNEUROSCI.4376-06.2007>
- Fouda, M.A., and P.C. Ruben. 2021. Protein kinases mediate anti-inflammatory effects of cannabidiol and estradiol against high glucose in cardiac sodium channels. *Front. Pharmacol.* 12:668657. <https://doi.org/10.3389/fphar.2021.668657>
- Fouda, M.A., M.R. Ghovanloo, and P.C. Ruben. 2020. Cannabidiol protects against high glucose-induced oxidative stress and cytotoxicity in cardiac voltage-gated sodium channels. *Br. J. Pharmacol.* 177:2932–2946. <https://doi.org/10.1111/bph.15020>
- Fouda, M.A., Y. Fathy Mohamed, R. Fernandez, and P.C. Ruben. 2022. Anti-inflammatory effects of cannabidiol against lipopolysaccharides in cardiac sodium channels. *Br. J. Pharmacol.* 179:5259–5272. <https://doi.org/10.1111/bph.15936>
- Fürst, O., and N. D'Avanzo. 2015. Isoform dependent regulation of human HCN channels by cholesterol. *Sci. Rep.* 5:14270. <https://doi.org/10.1038/srep14270>
- Ghovanloo, M.-R., N.G. Shuart, J. Mezeyova, R.A. Dean, P.C. Ruben, and S.J. Goodchild. 2018. Inhibitory effects of cannabidiol on voltage-dependent sodium currents. *J. Biol. Chem.* 293:16546–16558. <https://doi.org/10.1074/jbc.RA118.004929>
- Ghovanloo, M.R., K. Choudhury, T.S. Bandaru, M.A. Fouda, K. Rayani, R. Rusinova, T. Phaterpekar, K. Nelkenbrecher, A.R. Watkins, D. Poburko, et al. 2021. Cannabidiol inhibits the skeletal muscle Nav1.4 by blocking its pore and by altering membrane elasticity. *J. Gen. Physiol.* 153:e202012701. <https://doi.org/10.1085/jgp.202012701>
- Herrmann, S., B. Layh, and A. Ludwig. 2011. Novel insights into the distribution of cardiac HCN channels: An expression study in the mouse heart. *J. Mol. Cell. Cardiol.* 51:997–1006. <https://doi.org/10.1016/j.yjmcc.2011.09.005>
- Hill, A.J., C.M. Williams, B.J. Whalley, and G.J. Stephens. 2012. Phytocannabinoids as novel therapeutic agents in CNS disorders. *Pharmacol. Ther.* 133:79–97. <https://doi.org/10.1016/j.pharmthera.2011.09.002>
- Iffland, K., and F. Grotenhermen. 2017. An update on safety and side effects of cannabidiol: A review of clinical data and relevant animal studies. *Cannabis Cannabinoid Res.* 2:139–154. <https://doi.org/10.1089/can.2016.0034>
- Isaev, D., W. Shabbir, E.Y. Dinc, D.E. Lorke, G. Petroianu, and M. Oz. 2022. Cannabidiol inhibits multiple ion channels in rabbit ventricular cardiomyocytes. *Front. Pharmacol.* 13:821758. <https://doi.org/10.3389/fphar.2022.821758>
- Ishii, T.M., N. Nakashima, and H. Ohmori. 2007. Tryptophan-scanning mutagenesis in the S1 domain of mammalian HCN channel reveals residues critical for voltage-gated activation. *J. Physiol.* 579:291–301. <https://doi.org/10.1113/jphysiol.2006.124297>
- Jones, R.T. 2002. Cardiovascular system effects of marijuana. *J. Clin. Pharmacol.* 42:58S–63S. <https://doi.org/10.1002/j.1552-4604.2002.tb06004.x>
- Le Marois, M., V. Ballet, C. Sanson, M.A. Maizieres, T. Carriot, C. Chantoinseau, M. Partiseti, and G.A. Bohme. 2020. Cannabidiol inhibits multiple cardiac ion channels and shortens ventricular action potential duration in vitro. *Eur. J. Pharmacol.* 886:173542. <https://doi.org/10.1016/j.ejphar.2020.173542>
- Lee, C.-H., and R. MacKinnon. 2017. Structures of the human HCN1 hyperpolarization-activated channel. *Cell.* 168:111–120.e11. <https://doi.org/10.1016/j.cell.2016.12.023>
- Lee, C.-H., and R. MacKinnon. 2019. Voltage sensor movements during hyperpolarization in the HCN channel. *Cell.* 179:1582–1589.e7. <https://doi.org/10.1016/j.cell.2019.11.006>
- Lerner, M. 1963. Marijuana: Tetrahydrocannabinol and related compounds. *Science.* 140:175–176. <https://doi.org/10.1126/science.140.3563.175>
- Liang, Q., L. Yang, Z. Wang, S. Huang, S. Li, and G. Yang. 2009. Tanshinone IIA selectively enhances hyperpolarization-activated cyclic nucleotide-modulated (HCN) channel instantaneous current. *J. Pharmacol. Sci.* 110:381–388. <https://doi.org/10.1254/jphs.08334FP>
- Lolicato, M., M. Nardini, S. Gazzarrini, S. Möller, D. Bertinetti, F.W. Herberg, M. Bolognesi, H. Martin, M. Fasolini, J.A. Bertrand, et al. 2011. Tetramerization dynamics of C-terminal domain underlies isoform-specific cAMP gating in hyperpolarization-activated cyclic nucleotide-gated channels. *J. Biol. Chem.* 286:44811–44820. <https://doi.org/10.1074/jbc.M111.297606>
- Manne, J.R.R. 2018. A case of atenolol-induced sinus node dysfunction presenting as escape-capture bigeminy. *Oxf. Med. Case Rep.* 2018:omy015. <https://doi.org/10.1093/omcr/omy015>
- Margolis, J.R., H.C. Strauss, H.C. Miller, M. Gilbert, and A.G. Wallace. 1975. Digitalis and the sick sinus syndrome. Clinical and electrophysiologic documentation of severe toxic effect on sinus node function. *Circulation.* 52:162–169. <https://doi.org/10.1161/01.CIR.52.1.162>
- Mayar, S., M. Memarpoor-Yazdi, A. Makky, R. Eslami Sarokhalil, and N. D'Avanzo. 2022. Direct regulation of hyperpolarization-activated cyclic-nucleotide gated (HCN1) channels by cannabinoids. *Front. Mol. Neurosci.* 15:848540. <https://doi.org/10.3389/fnmol.2022.848540>
- Moosmang, S., J. Stieber, X. Zong, M. Biel, F. Hofmann, and A. Ludwig. 2001. Cellular expression and functional characterization of four hyperpolarization-activated pacemaker channels in cardiac and neuronal tissues. *Eur. J. Biochem.* 268:1646–1652. <https://doi.org/10.1046/j.1432-1327.2001.02036.x>
- Novella Romanelli, M., L. Sartiani, A. Masi, G. Mannaioni, D. Manetti, A. Mugelli, and E. Cerbai. 2016. HCN channels modulators: The need for selectivity. *Curr. Top. Med. Chem.* 16:1764–1791. <https://doi.org/10.2174/1568026616999160315130832>
- Ono, K., H.A. Fozzard, and D.A. Hanck. 1993. Mechanism of cAMP-dependent modulation of cardiac sodium channel current kinetics. *Circ. Res.* 72:807–815. <https://doi.org/10.1161/01.RES.72.4.807>
- Orvos, P., B. Pászti, L. Topal, P. Gazdag, J. Prorok, A. Polyák, T. Kiss, E. Tóth-Molnár, B. Csupor-Löffler, Á. Bajtel, et al. 2020. The electrophysiologic effect of cannabidiol on hERG current and in Guinea-pig and rabbit

- cardiac preparations. *Sci. Rep.* 10:16079. <https://doi.org/10.1038/s41598-020-73165-2>
- Page, D.A., K.E.A. Magee, J. Li, M. Jung, and E.C. Young. 2020. Cytoplasmic autoinhibition in HCN channels is regulated by the transmembrane region. *J. Membr. Biol.* 253:153–166. <https://doi.org/10.1007/s00232-020-00111-8>
- Pian, P., A. Bucchi, R.B. Robinson, and S.A. Siegelbaum. 2006. Regulation of gating and rundown of HCN hyperpolarization-activated channels by exogenous and endogenous PIP₂. *J. Gen. Physiol.* 128:593–604. <https://doi.org/10.1085/jgp.200609648>
- Pian, P., A. Bucchi, A. Decostanzo, R.B. Robinson, and S.A. Siegelbaum. 2007. Modulation of cyclic nucleotide-regulated HCN channels by PIP₂ and receptors coupled to phospholipase C. *Pflugers Arch.* 455:125–145. <https://doi.org/10.1007/s00424-007-0295-2>
- Porro, A., A. Saponaro, F. Gasparri, D. Bauer, C. Gross, M. Pisoni, G. Abbandonato, K. Hamacher, B. Santoro, G. Thiel, and A. Moroni. 2019. The HCN domain couples voltage gating and cAMP response in hyperpolarization-activated cyclic nucleotide-gated channels. *Elife*. 8:e49672. <https://doi.org/10.7554/eLife.49672>
- Postea, O., and M. Biel. 2011. Exploring HCN channels as novel drug targets. *Nat. Rev. Drug Discov.* 10:903–914. <https://doi.org/10.1038/nrd3576>
- Ramentol, R., M.E. Perez, and H.P. Larsson. 2020. Gating mechanism of hyperpolarization-activated HCN pacemaker channels. *Nat. Commun.* 11:1419. <https://doi.org/10.1038/s41467-020-15233-9>
- Rozario, A.O., H.K. Turbendian, K.J. Fogle, N.B. Olivier, and G.R. Tibbs. 2009. Voltage-dependent opening of HCN channels: Facilitation or inhibition by the phytoestrogen, genistein, is determined by the activation status of the cyclic nucleotide gating ring. *Biochim. Biophys. Acta.* 1788:1939–1949. <https://doi.org/10.1016/j.bbame.2009.06.003>
- Sait, L.G., A. Sula, M.R. Ghovanloo, D. Hollingworth, P.C. Ruben, and B.A. Wallace. 2020. Cannabidiol interactions with voltage-gated sodium channels. *Elife*. 9:1–17. <https://doi.org/10.7554/eLife.58593>
- Saponaro, A., D. Bauer, M.H. Giese, P. Swuec, A. Porro, F. Gasparri, A.S. Sharifzadeh, A. Chaves-Sanjuan, L. Alberio, G. Parisi, et al. 2021. Gating movements and ion permeation in HCN4 pacemaker channels. *Mol. Cell.* 81:2929–2943.e6. <https://doi.org/10.1016/j.molcel.2021.05.033>
- Scheffer, I.E., J.J. Halford, I. Miller, R. Nabbout, R. Sanchez-Carpintero, Y. Shiloh-Malawsky, M. Wong, M. Zolnowska, D. Checketts, E. Dunayevich, and O. Devinsky. 2021. Add-on cannabidiol in patients with Dravet syndrome: Results of a long-term open-label extension trial. *Epilepsia.* 62:2505–2517. <https://doi.org/10.1111/epi.17036>
- Schweizer, P.A., N. Duhme, D. Thomas, R. Becker, J. Zehelein, A. Draguhn, C. Bruehl, H.A. Katus, and M. Koenen. 2010. cAMP sensitivity of HCN pacemaker channels determines basal heart rate but is not critical for autonomic rate control. *Circ. Arrhythm. Electrophysiol.* 3:542–552. <https://doi.org/10.1161/CIRCEP.110.949768>
- Shi, W., R. Wymore, H. Yu, J. Wu, R.T. Wymore, Z. Pan, R.B. Robinson, J.E. Dixon, D. McKinnon, and I.S. Cohen. 1999. Distribution and prevalence of hyperpolarization-activated cation channel (HCN) mRNA expression in cardiac tissues. *Circ. Res.* 85:e1–e6. <https://doi.org/10.1161/01.res.85.1.e1>
- Stanley, C.P., W.H. Hind, and S.E. O'Sullivan. 2013. Is the cardiovascular system a therapeutic target for cannabidiol? *Br. J. Clin. Pharmacol.* 75:313–322. <https://doi.org/10.1111/j.1365-2125.2012.04351.x>
- Stieber, J., A. Thomer, B. Much, A. Schneider, M. Biel, and F. Hofmann. 2003. Molecular basis for the different activation kinetics of the pacemaker channels HCN2 and HCN4. *J. Biol. Chem.* 278:33672–33680. <https://doi.org/10.1074/jbc.M305318200>
- Strauss, H.C., M. Gilbert, R.H. Svenson, H.C. Miller, and A.G. Wallace. 1976. Electrophysiologic effects of propranolol on sinus node function in patients with sinus node dysfunction. *Circulation.* 54:452–459. <https://doi.org/10.1161/01.CIR.54.3.452>
- Tao, X., A. Lee, W. Limapichat, D.A. Dougherty, and R. MacKinnon. 2010. A gating charge transfer center in voltage sensors. *Science.* 328:67–73. <https://doi.org/10.1126/science.1185954>
- Topal, L., M. Naveed, P. Orvos, B. Pászti, J. Prorok, Á. Bajtel, T. Kiss, B. Csopor-Löffler, D. Csopor, I. Baczkó, et al. 2021. The electrophysiological effects of cannabidiol on action potentials and transmembrane potassium currents in rabbit and dog cardiac ventricular preparations. *Arch. Toxicol.* 95:2497–2505. <https://doi.org/10.1007/s00204-021-03086-0>
- Trott, O., and A.J. Olson. 2010. AutoDock Vina: Improving the speed and accuracy of docking with a new scoring function, efficient optimization, and multithreading. *J. Comput. Chem.* 31:455–461. <https://doi.org/10.1002/jcc.21334>
- Ueda, K., Y. Hirano, Y. Higashiuesato, Y. Aizawa, T. Hayashi, N. Inagaki, T. Tana, Y. Ohya, S. Takishita, H. Muratani, et al. 2009. Role of HCN4 channel in preventing ventricular arrhythmia. *J. Hum. Genet.* 54:115–121. <https://doi.org/10.1038/jhg.2008.16>
- Wahl-Schott, C., and M. Biel. 2009. HCN channels: Structure, cellular regulation and physiological function. *Cell. Mol. Life Sci.* 66:470–494. <https://doi.org/10.1007/s00018-008-8525-0>
- Wainger, B.J., M. DeGennaro, B. Santoro, S.A. Siegelbaum, and G.R. Tibbs. 2001. Molecular mechanism of cAMP modulation of HCN pacemaker channels. *Nature.* 411:805–810. <https://doi.org/10.1038/35081088>
- Walsh, S.K., C.Y. Hepburn, K.A. Kane, and C.L. Wainwright. 2010. Acute administration of cannabidiol in vivo suppresses ischaemia-induced cardiac arrhythmias and reduces infarct size when given at reperfusion. *Br. J. Pharmacol.* 160:1234–1242. <https://doi.org/10.1111/j.1476-5381.2010.00755.x>
- Wang, J., S. Chen, and S.A. Siegelbaum. 2001. Regulation of hyperpolarization-activated HCN channel gating and cAMP modulation due to interactions of COOH terminus and core transmembrane regions. *J. Gen. Physiol.* 118:237–250. <https://doi.org/10.1085/jgp.118.3.237>
- Xu, X., Z.V. Vysotskaya, Q. Liu, and L. Zhou. 2010. Structural basis for the cAMP-dependent gating in the human HCN4 channel. *J. Biol. Chem.* 285:37082–37091. <https://doi.org/10.1074/jbc.M110.152033>
- Zagotta, W.N., N.B. Olivier, K.D. Black, E.C. Young, R. Olson, and E. Gouaux. 2003. Structural basis for modulation and agonist specificity of HCN pacemaker channels. *Nature.* 425:200–205. <https://doi.org/10.1038/nature01922>
- Zhang, Q., A. Huang, Y.C. Lin, and H.G. Yu. 2009. Associated changes in HCN2 and HCN4 transcripts and I(f) pacemaker current in myocytes. *Biochim. Biophys. Acta.* 1788:1138–1147. <https://doi.org/10.1016/j.bbame.2009.02.011>
- Zhang, H.B., L. Heckman, Z. Niday, S. Jo, A. Fujita, J. Shim, R. Pandey, H. Al Jandal, S. Jayakar, L.B. Barrett, et al. 2022. Cannabidiol activates neuronal Kv7 channels. *Elife*. 11:1–15. <https://doi.org/10.7554/eLife.73246>
- Zolles, G., N. Klöcker, D. Wenzel, J. Weisser-Thomas, B.K. Fleischmann, J. Roeper, and B. Fakler. 2006a. Pacemaking by HCN channels requires interaction with phosphoinositides. *Neuron.* 52:1027–1036. <https://doi.org/10.1016/j.neuron.2006.12.005>

Supplemental material

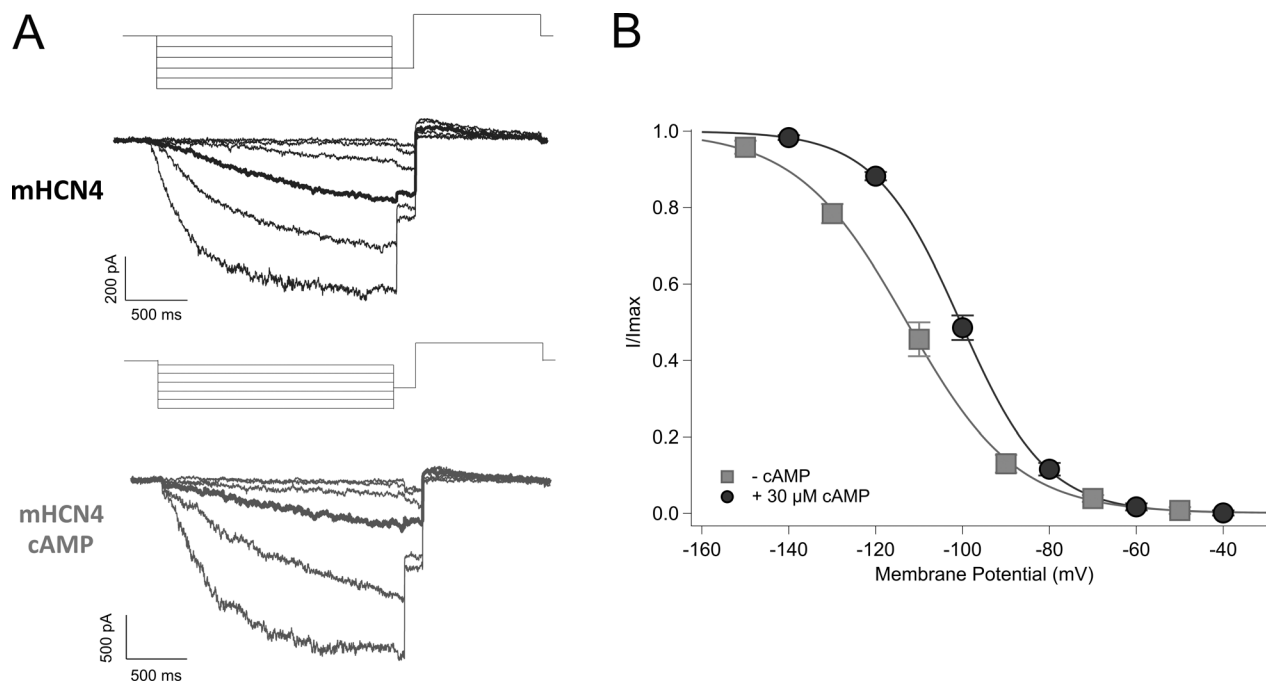


Figure S1. **Effect of cAMP on HCN4 channels.** **(A)** Representative voltage protocol and activation current traces for mHCN4 without cAMP (i.e., apo) (grey, above) and mHCN4 with 30 μ M cAMP (i.e., holo) (black, below). **(B)** Average tail current values for treatment with apo HCN4 (grey square) and holo HCN4 (30 μ M cAMP) (black circle). Values fit to a Boltzmann curve. Average $V_{1/2}$ for apo HCN4 was -113.2 ± 2.2 mV ($n = 7$); average $V_{1/2}$ for holo HCN4 was -101.74 ± 0.75 mV ($n = 39$).

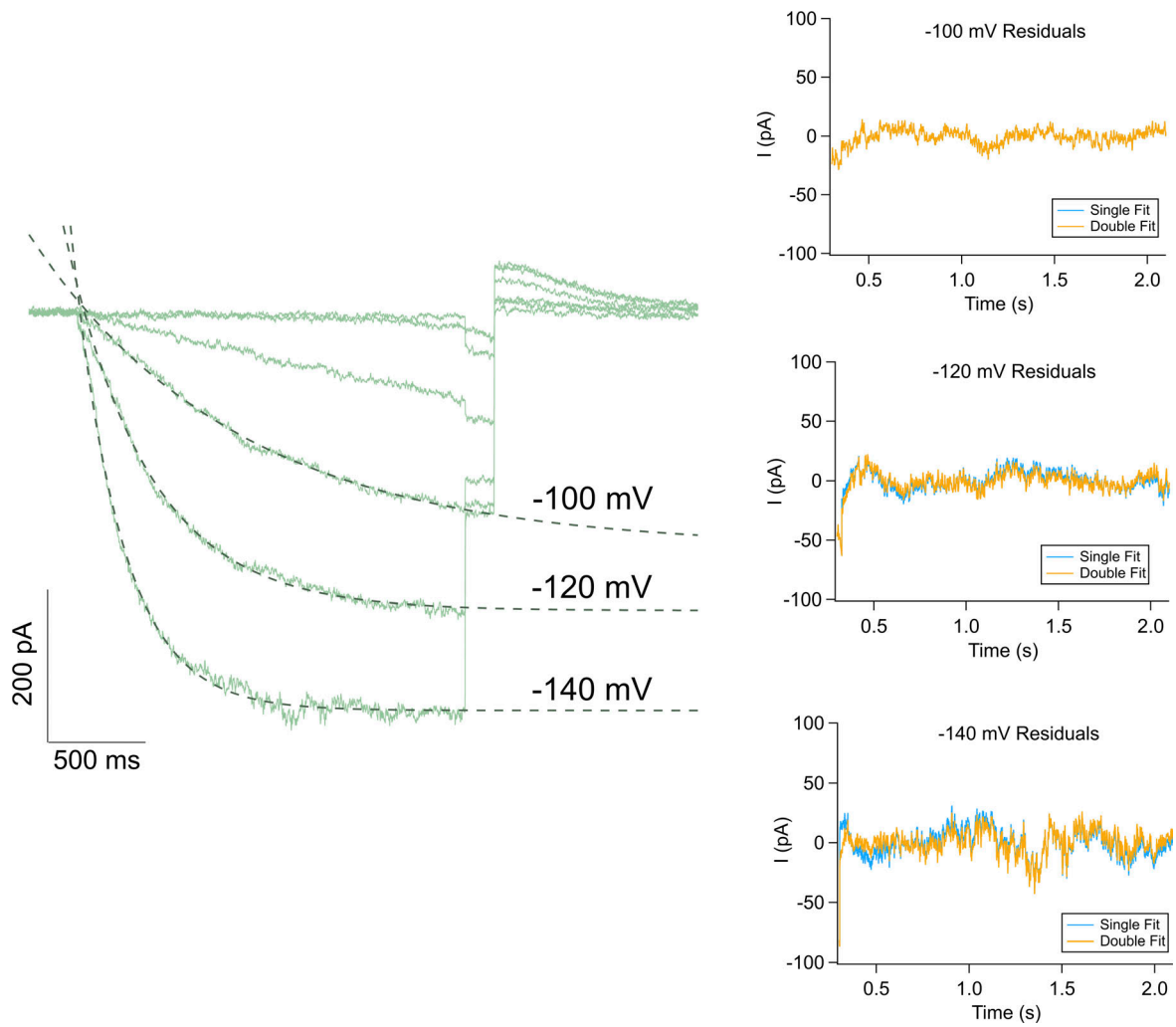
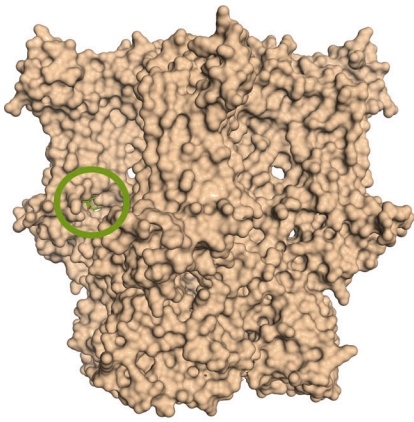
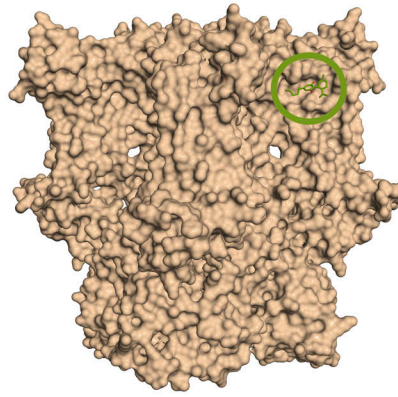


Figure S2. **Comparison of single and double exponential fits.** Left: Representative trace of holo mHCN4 after application of 5 μ M CBD (green). Single exponential fits for -100, -120, and -140 mV traces shown as a dashed line. Right: Comparison of residuals from single (blue) and double (orange) exponential fits for a representative trace shown to left. Based on the lack of change in residuals with increase to a double exponential equation, single exponential fits were deemed sufficient to describe the activation curves.



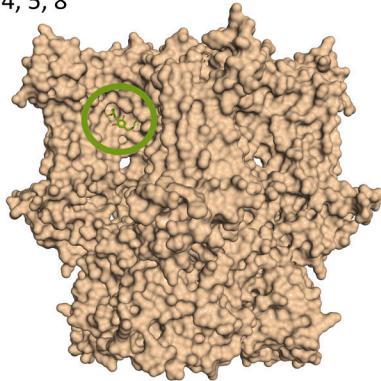
S4 pocket:

Tetramer Computed binding sites 1 (B), 2 (D), 7 (D), 8 (C), 9 (B)
 Monomer Computed binding sites 1, 3, 4, 5, 8



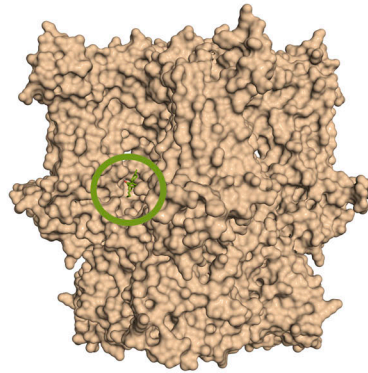
S1 C-term:

Tetramer Computed binding sites 3 (B), 4 (A), 5 (D), 6 (C)
 Monomer Computed binding sites 2, 6



VSD-Pore Interface

Monomer Computed binding site 7



S4-S5 linker:

Monomer Computed binding site 9

Tetramer Calculation

Mode	Affinity (kcal/mol)
------	---------------------

1	-7.4
2	-7.4
3	-7.2
4	-7.2
5	-7.2
6	-7.2
7	-7.2
8	-7.1
9	-7.1

Monomer Calculation

Mode	Affinity (kcal/mol)
------	---------------------

1	-7.4
2	-7.2
3	-7.1
4	-7.0
5	-7.0
6	-6.9
7	-6.9
8	-6.8
9	-6.8

Figure S3. **General regions for CBD (green) binding on an HCN4 cyroEM structure (PDB ID 7NP4).** Calculated affinities for tetramer and monomer calculations listed on the right. Computed using AutoDock Vina, with exhaustiveness set to 1,000 for tetramer, 100 for monomer.

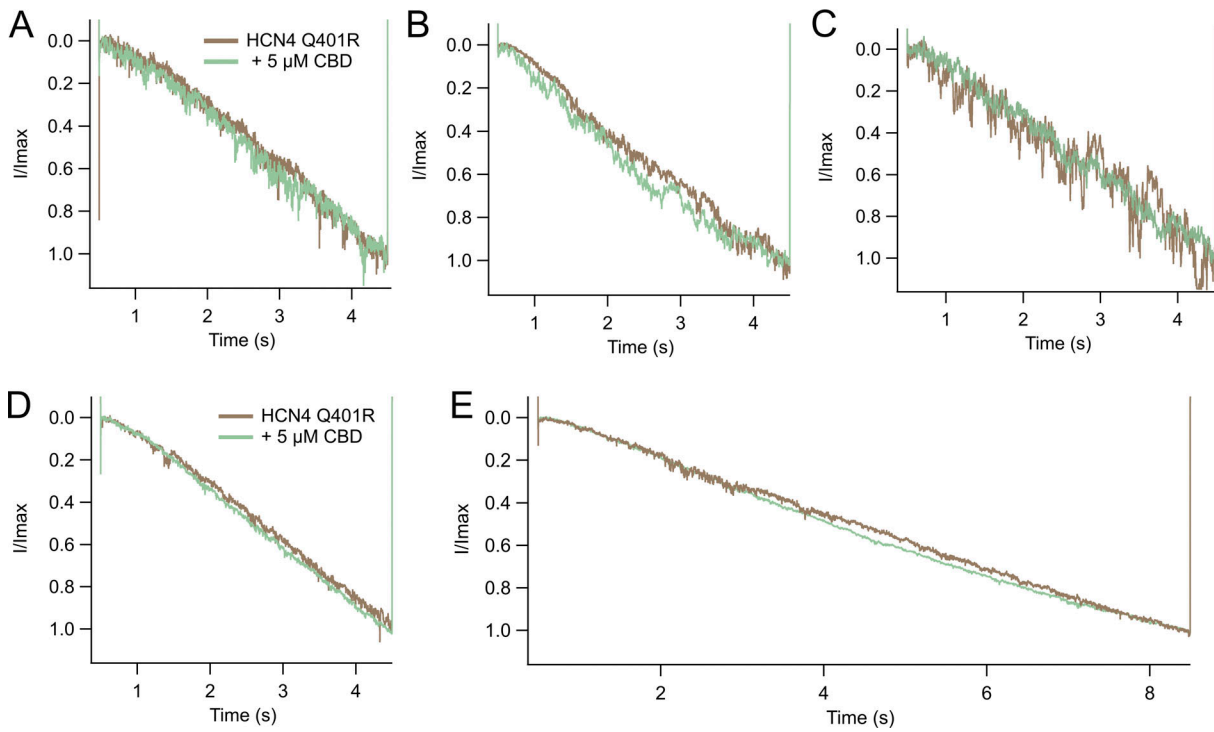
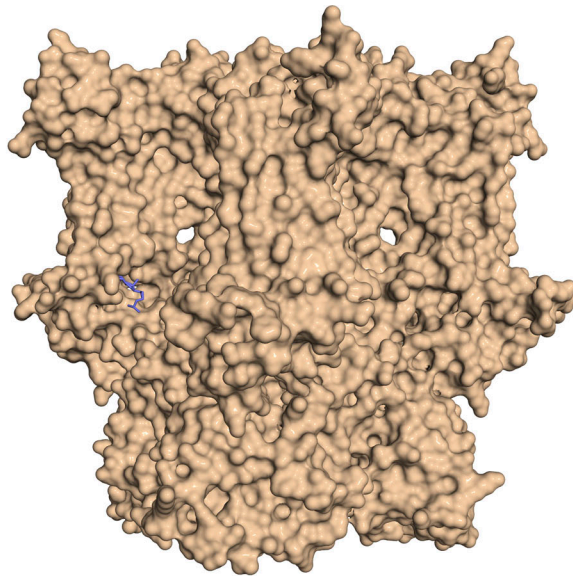
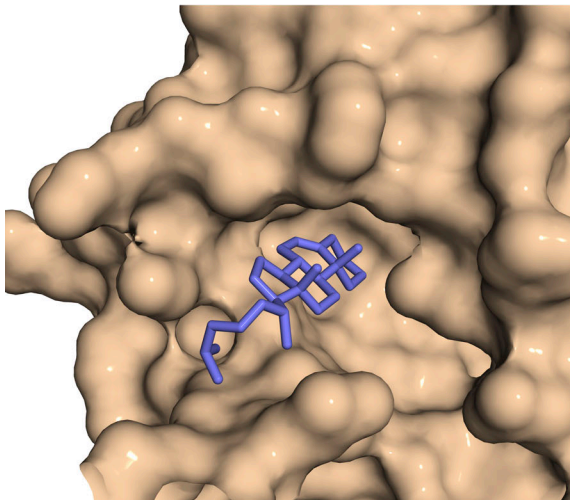


Figure S4. **CBD does not speed HCN4 Q401R activation.** Representative traces were normalized to peak current and superimposed before (brown) and after (green) application of 5 μM CBD. **(A–D)** Out of a total of eight cells, four were chosen as representatives (A–D) across three separate transfections. D was chosen as the representative trace shown in Fig. 4 E. **(E)** The same cell as in D is shown after activation time from D was doubled to 8 s.



Cholesterol
binding site #1
(7.5 kcal/mol)



Cholesterol
binding site #1
zoom in

Figure S5. **Highest affinity binding site for cholesterol (blue) on HCN4 (PDB ID 7NP4) in the S4 lipid pocket.** Calculated with AutoDock Vina.